



# Novel electrochemical sensor based on polydopamine molecularly imprinted polymer for sensitive and selective detection of *Acinetobacter baumannii*

Mahmoud Roushani<sup>1</sup> · Masoumeh Sarabaegi<sup>1</sup> · Arman Rostamzad<sup>2</sup>

Received: 18 February 2020 / Accepted: 10 April 2020 / Published online: 24 April 2020  
© Iranian Chemical Society 2020

## Abstract

*Acinetobacter baumannii* (*A. baumannii*) which is one of the most problematic causative agents of nosocomial infections, worldwide, can severely cause morbidity and mortality within the healthcare community and present a particular threat to intensive care unit patients. The infection caused by these bacteria strains is a major cause for concern among healthcare professionals and is prompting changes in both antibiotic regimens and hospital disinfection techniques. Different protocols have been employed for the identification of samples or hospital equipment, colonized by *A. baumannii*, so that appropriate decontamination procedures can be carried out. In this work, we introduced a new diagnostic test for *A. baumannii* with a molecularly imprinted polymer (MIP). The MIP was carried out on the surface of the glassy carbon electrode applying the electropolymerization of the dopamine monomer with the template of *A. baumannii*. The electrochemical techniques, such as cyclic voltammetry and impedance spectroscopy, were performed in order to characterize the NIP and MIP modified electrode in the hexacyanoferrate redox system as an electrochemical probe. The sensor exhibited a linear range of  $10^2$ – $10^7$  CFU L<sup>-1</sup> for detecting *A. baumannii* with a detection limit of 30 CFU L<sup>-1</sup>. This sensor was successfully used to test the recovery of *A. baumannii* in human blood serum samples. According to our knowledge, this is the first report on a MIP sensor to detect *A. baumannii*.

**Keywords** Impedimetric detection · Molecularly imprinted polymer · Polydopamine · *Acinetobacter baumannii*

## Introduction

One of the members of the genus *Acinetobacter*, *A. baumannii*, has recently been recognized as the main cause of antibiotic-resistant infections. Moreover, such resisting species can lead to an outbreak in local diseases and environmental pollution and can also play an important role in this outbreak. *A. baumannii* which is one of the worst pathogens in hospitals spreads infection at intensive care unit (ICU) around the world [1–4]. The global mortality caused by *A. baumannii* in 2014 was approximately 35% [5]. The methods for the detection and identification of *A. baumannii* mainly

include polymerase chain reactions (PCR) [6], culture-based assays [7], mass spectrometry [8] and fluorescence [9]. However, these methods are often time-consuming and difficult. Some patients lost the best treatment because they failed receiving prompt diagnosis. Therefore, finding a simple method and saving time are vital for the diagnosis of *A. baumannii*.

Lately, a combination of the molecularly imprinted technology with an electrochemical sensor, an important molecular diagnostic tool for increasing the ability to select electrochemical sensors, has been reported to be a good design strategy [10, 11]. MIP has sites that are highly selective ones containing the target molecule [12]. In this sense, MIP is becoming an important analytical tool [13]. Moreover, MIP is polymerized in the presence of target molecules known as composite materials and has specific bonding sites for the targeting molecules [14]. After removing the target molecules by removing the physical methods or chemical elution, binding sites within the MIP become complementary, in structure and size, to the target

✉ Mahmoud Roushani  
mahmoudroushani@yahoo.com; m.roushani@ilam.ac.ir

<sup>1</sup> Department of Chemistry, Faculty of Sciences, Ilam University, P. O. Box 69315-516, Ilam, Iran

<sup>2</sup> Department of Biology, Faculty of Sciences, Ilam University, P. O. Box 69315-516, Ilam, Iran

molecules to the extent that can specifically detect the target molecules [15, 16]. As compared to other techniques, electro-polymerization is remarkable for electrochemical analysis due to its good reproducibility and ease of preparation [17, 18]. In this sense, a wide range of molecules and macromolecules can be imprinted [19–21]. In this research, the electrochemical sensor based on *A. baumannii*-imprinted polydopamine(PDA) was described. This sensor was a very selective and sensitive electrochemical sensor for *A. baumannii* in the real sample.

## Experimental

### Instruments and reagents

Dopamine and  $K_4[Fe(CN)_6]/K_3[Fe(CN)_6]$  were used without any further purification, and all other reagents were purchased from Merck ([www.merck.com](http://www.merck.com)) or Fluka. *A. baumannii*, *Escherichia coli*, *Klebsiella pneumoniae*, *Salmonella enteritidis*, *Pseudomonas aeruginosa* and *Shigella flexneri* were provided by the Department of Microbiology Ilam University, Iran.

Differential pulse voltammetry (DPV), cyclic voltammetry (CV) and impedance spectroscopy (EIS) measurements were carried out with  $\mu$ -AUTOLAB electrochemical analysis. In all experiments, a solution in  $0.1 \text{ mol L}^{-1}$  KCl,  $5 \text{ mmol L}^{-1}$   $[Fe(CN)_6]^{3-/4-}$  was used. Ag/AgCl electrode as the reference, a modified glassy carbon electrode (GCE) as the working electrode and a platinum wire as the counter electrode were used. EIS measurements were used within the frequency range of 0.1–10 kHz with 5 mV amplitude. Field

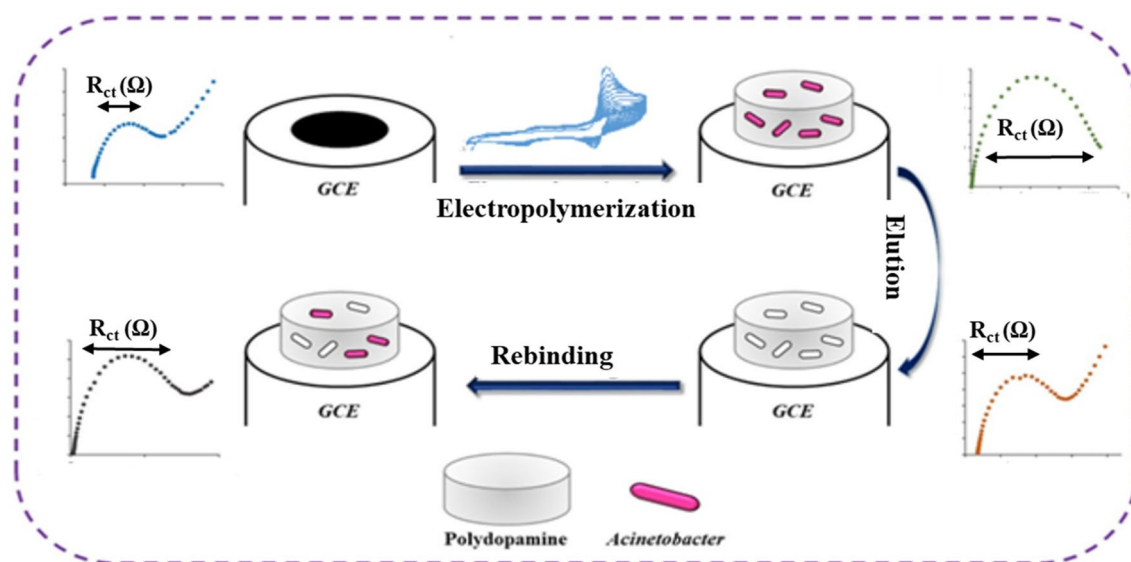
emission scanning electron microscopy (FE-SEM) was used to study the surface morphology of the samples (Model: Hitachi S4160).

### Preparation of the sensors molecularly imprinted polymer

The GCE was cleaned with alumina powder. The GCE was then sonicated in a mixture of water and ethanol. During the next stage, the bare GCE was performed by the polymerization of dopamine monomer according to the article [22]. Briefly, electropolymerizing conditions were performed to phosphate buffer (PB) solution (pH 7.4), containing 0.05 M dopamine and  $10^7 \text{ CFU L}^{-1}$  *A. baumannii*, which was then degassed with nitrogen for 10 min. Electropolymerization was performed using cyclic voltammetry by 13 cycles,  $-0.5$  to  $0.5 \text{ V}$  versus Ag/AgCl, scan rate of  $20 \text{ mV s}^{-1}$ . Finally, electrodes were rinsed with water and, then, washed 2 h in order to remove the template in the washing solution ( $0.01 \text{ M}$  SDS and  $10 \text{ mM}$   $HNO_3$  in water) with stirring. As a control, a non-imprinted polymer modified electrode (NIP) was prepared in accordance with the same method and without the template. The schematic representation for the fabricated MIP and the assay protocol for *A. baumannii* detection were given in Scheme 1.

### Bacteria preparation

A fresh colony from each bacterial was taken and cultured on Luria–Bertani (*LB*) broth and, then, incubated at  $37 \text{ }^\circ\text{C}$  for 18 h. Afterward, the concentration of the culture was



**Scheme 1** The electrochemical polymerization of the MIP film, the elution and detection process of the sensor

adjusted to 0.5 McFarland turbidity ( $10^7$  bacteria) in mL. The serial dilution ( $10^2$ ,  $10^3$ ,  $10^4$ ,  $10^5$ ,  $10^6$  and  $10^7$ ) was made using PB solution (pH 7.4). Moreover, *P. aeruginosa*, *E. coli*, *S. enteritidis*, *S. flexneri* and *K. pneumoniae* were used to investigate the sensor specificity.

## Results and discussion

### Electrochemical characterization

The step-by-step morphological structures of the electrodes modified by FE-SEM were investigated. As shown in Fig. 1a, the FE-SEM displays a uniform MIP film distributed on the surface of the electrode. Figure 1b illustrates that after washing *A. baumannii* at the MIP/GCE surface, the SEM image of the electrode was obtained with many pores in the MIP/GCE surface.

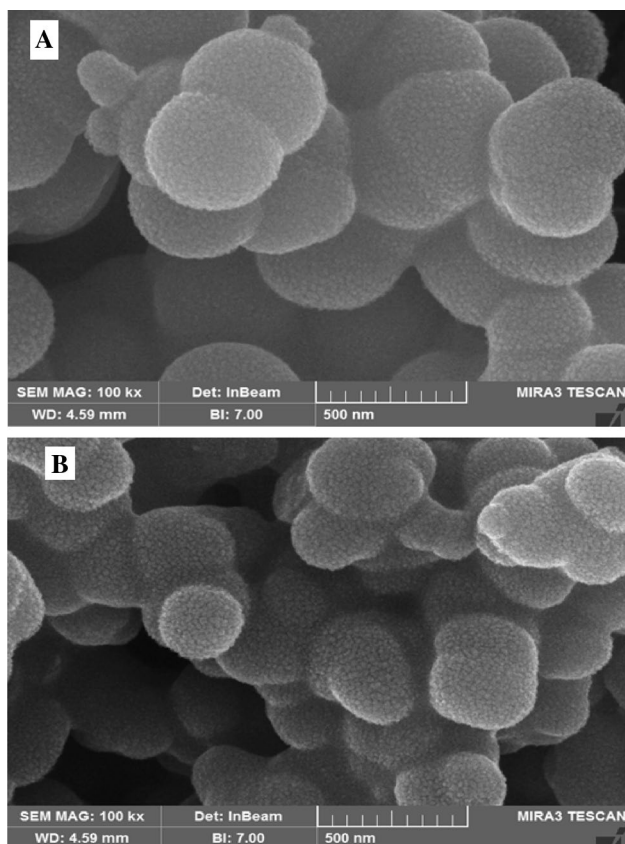
The CV technique was described for the electrochemical behavior of MIP/GCE and NIP/GCE in solutions containing 5.0 mM  $K_3[Fe(CN)_6]/K_4[Fe(CN)_6]$  and 0.1 M KCl (Fig. 2a). In this sense, the bare GCE illustrates (curve a). After electropolymerization, the peak current decreased significantly

(curve b). This shows that the polymerization has occurred. When the modified electrode was immersed in sodium dodecyl sulfate (SDS) (0.01 M)/ $HNO_3$  (10 mM) for 2 h, outgrowing peaks for  $[Fe(CN)_6]^{3-}/[Fe(CN)_6]^{4-}$  were improved because the cavity has been created on the surface of the electrode resulting from the removal of the template (curve c). The electrochemical behavior of the  $[Fe(CN)_6]^{3-}/[Fe(CN)_6]^{4-}$ , after removal, on NIP/GCE was also investigated. As shown in (curve d), the NIP/GCE curves have no apparent differences. After incubating the MIP/GCE in *A. baumannii*  $10^2$  CFU  $mL^{-1}$  solution for 70 min, *A. baumannii* was again absorbed into the copolymer film and, then, the peak current decreased (curve e).

EIS is an efficient tool for studying the interface properties of the modified electrodes; the half-rotating impedance diameter is equal to the electron-transfer resistance ( $R_{ct}$ ). Figure 2b shows the EIS of (curve a) the bare GCE. In addition, after electropolymerization, a very high-frequency semicircle (curve b) was obtained. This may indicate that there is a non-conductive layer on the surface of the electrode (MIP/GCE). When *A. baumannii* was removed from the electrode surface, by the washing solution, the semicircular resistance was decreased. This means that the electron-transfer has become easier as pores at about the size of *A. baumannii* were created on the surface of the modified electrode (curve c). The electrochemical behavior of the  $[Fe(CN)_6]^{3-}/[Fe(CN)_6]^{4-}$ , after the removal on NIP/GCE, was not changed in a semicircle frequency as it was similar to (curve d). Afterward, the semicircle increased after rebinding the template in the MIP (curve d), indicating that the MIP film was successfully prepared. These results are consistent with the CV curve and confirm that there are cavities formed during the electropolymerization in the presence of the template.

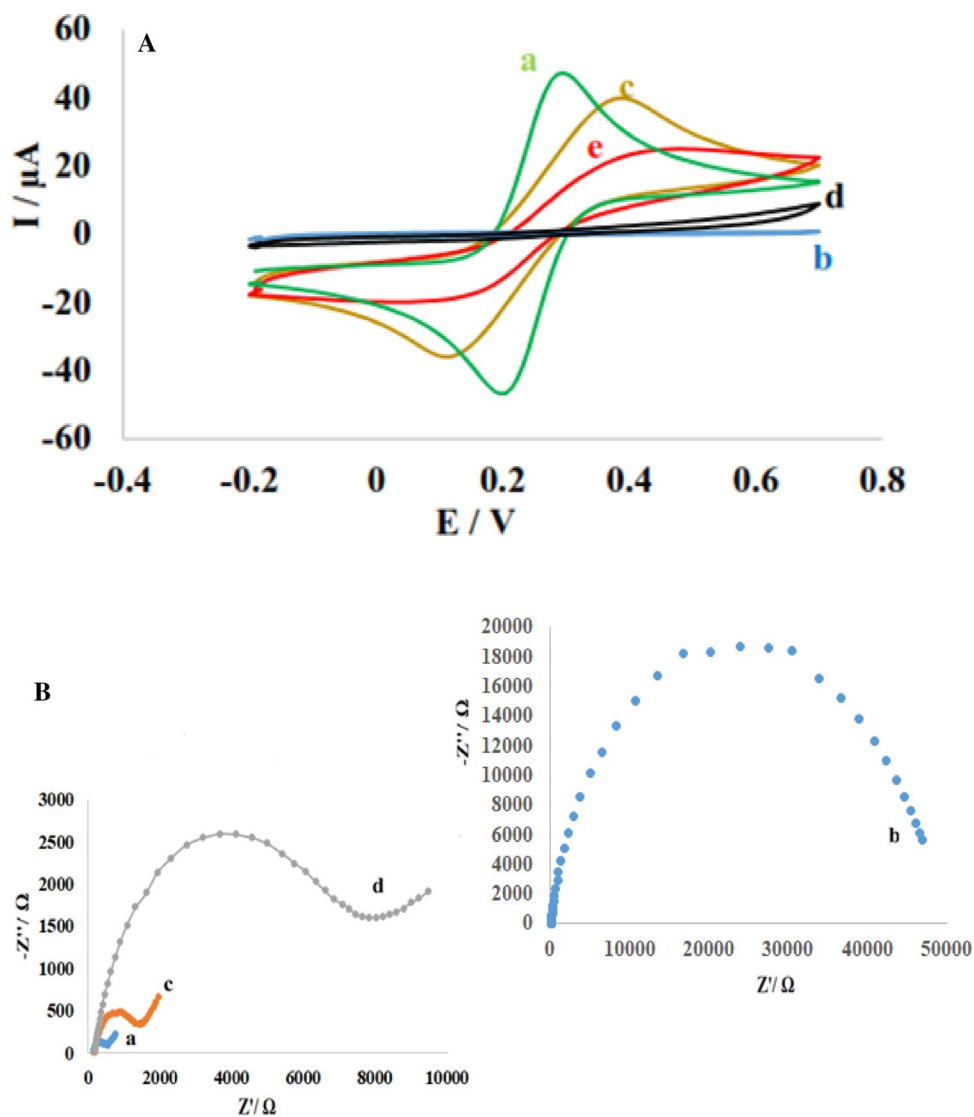
### Electrochemical response of the proposed MIP to *A. baumannii*

Under the optimized experimental conditions, the MIP response to an increase in the concentration of *A. baumannii* is shown. As seen in Fig. 3a, increasing the concentration of *A. baumannii* increases the semicircular resistance ( $R_{ct}$ ). According to the concentration of *A. baumannii* in a linear range;  $10^2$  to  $10^7$  CFU  $mL^{-1}$ , the linear equation could be depicted as  $\Delta R_{ct} = 5.7755 [A. baumannii] (CFU ml^{-1}) + 2.1669$ , the correlation coefficient ( $R^2$ ) was 0.9726 and its detection limit was 30 CFU  $mL^{-1}$  as shown in Fig. 3b (based on  $S/N=3$ ). In this sense, it is in Table 1 that the sensor is compared to other methods for the detection of *A. baumannii*.

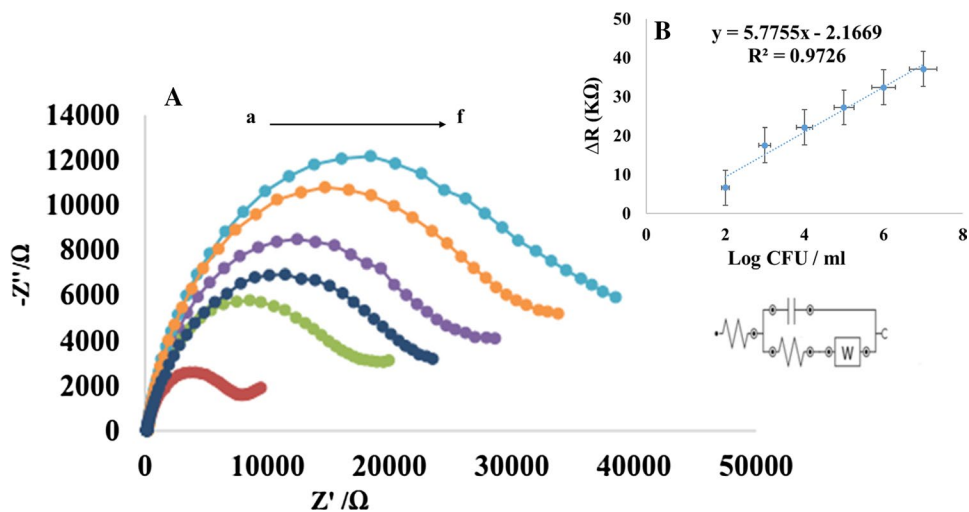


**Fig. 1** SEM photographs of the MIP/GCE before (a) and after (b) elution the *A. baumannii*

**Fig. 2** (A) CV results of bare GCE (a), dopamine electropolymerization (b), the *A. baumannii* were removed (c), NIP/GCE after in anelution (d), and MIP/GCE after rebinding with *A. baumannii* (e). (B) Nyquist plots of bare GCE (a), dopamine electropolymerization (b), the *A. baumannii* was removed (c) and MIP/GCE after rebinding with *A. baumannii* (d). In a 0.1 M KCl, 5 mM of  $[\text{Fe}(\text{CN})_6]^{3-/4-}$  solutions

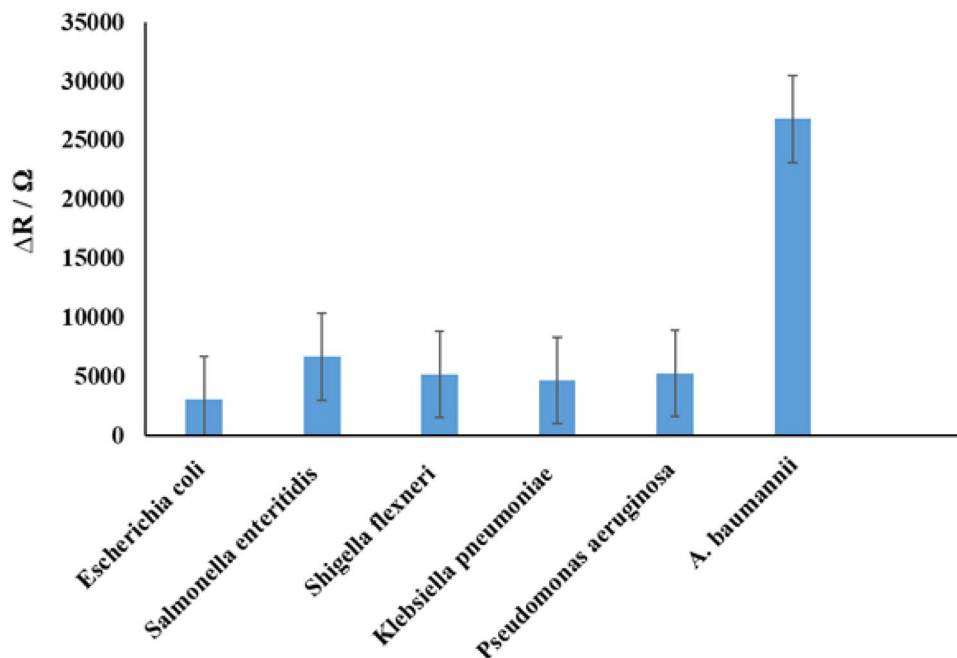


**Fig. 3** EIS results for the MIP/GCE exposed with different concentration of *A. baumannii* including (a)  $10^2$ , (b)  $10^3$ , (c)  $10^4$ , (d)  $10^5$ , (e)  $10^6$  and (f)  $10^7$  CFU  $\text{mL}^{-1}$  and its calibration plot for  $\Delta R$  versus Log (concentration) of *A. baumannii* in 5.0 mM  $\text{K}_3[\text{Fe}(\text{CN})_6]/\text{K}_4[\text{Fe}(\text{CN})_6]$  (1:1) in 0.1 mol  $\text{L}^{-1}$  KCl. EIS was performed in a frequency range of 100 kHz to 0.05 Hz ( $E_{\text{DC}} = 0.23$  V)



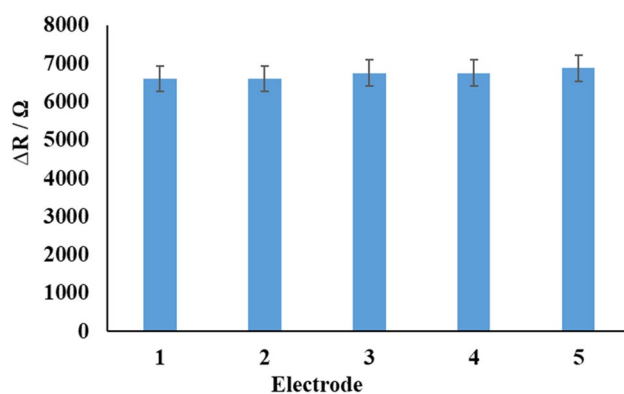
**Table 1** Comparison of the method with other methods for detection of *A. baumannii*

Method	Linear dynamic range (CFU mL <sup>-1</sup> )	LOD (CFU mL <sup>-1</sup> ) colony-forming-unit	Reference
Fluorescence	1 × 10 <sup>4</sup> –5 × 10 <sup>7</sup>	2.3 × 10 <sup>3</sup>	[9]
Aptamer assay		100	[23]
Tail fiber protein-immobilized magnetic nanoparticle		10 <sup>4</sup> –10 <sup>5</sup>	[24]
In this study	10 <sup>2</sup> –10 <sup>7</sup>	30	–

**Fig. 4** Selectivity of the MIP/GCE sensor for *A. baumannii* detection. EIS response of the MIP/GCE incubated in 10<sup>5</sup> CFU mL<sup>-1</sup> solutions of *A. baumannii*, *P. aeruginosa*, *S. flexneri*, *S. enteritidis*, *E. coli* and *K. pneumoniae*. Conditions: all of the bacterial solutions were prepared in PB solutions (0.1 mol L<sup>-1</sup>, pH 7.4)

### Selectivity, repeatability and incubation time of the sensor

The selective method is very important in an electrochemical sensor for template recognition and the detection based on molecularly imprinted polymer. Herein, 10<sup>5</sup> CFU mL<sup>-1</sup> solutions of *P. aeruginosa*, *E. coli*, *K. pneumoniae*, *S. enteritidis* and *S. flexneri* are chosen to check the selectivity in this sensor. As shown in Fig. 4, the response of *A. baumannii* at MIP/GCE electrode indicated that *A. baumannii* can be detected in the presence of other bacteria. The repeatability of the sensor was investigated using the EIS method in 5.0 mM K<sub>3</sub>[Fe(CN)<sub>6</sub>]/K<sub>4</sub>[Fe(CN)<sub>6</sub>] redox probe. This sensor was immersed in 10<sup>2</sup> CFU mL<sup>-1</sup> *A. baumannii* solution and repeated for 5 electrodes. The relative standard deviation (RSD) of 4.2% was calculated for the sensor, which showed the appropriate value Fig. 5. In order to measure the effects of incubation, the time span from 0.5 to 3 h was studied. In an incubation time from 0.5 to 2 h, DPV response increased and, then, remained constant as shown in Fig. 6.

**Fig. 5** Histogram of the ΔR response for 5 electrodes which modified under the same conditions (5 mmol L<sup>-1</sup> [Fe(CN)<sub>6</sub>]<sup>3-/4-</sup> (1:1) in 0.1 mol L<sup>-1</sup> KCl. E<sub>DC</sub>=0.23 V). The error bars represent the standard deviation of three experiments

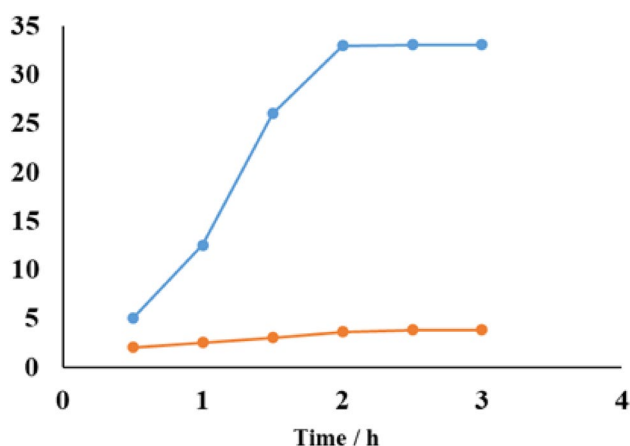


**Fig. 6** Influence of elution time in 0.01 M SDS and 10 mM HNO<sub>3</sub> in water on the response of **a** MIP/GCE **b** NIP/GCE sensor in 5 mM [Fe(CN)<sub>6</sub>]<sup>3-/4-</sup> solution

**Table 2** Detection of *A. baumannii* in some real samples ( $n=3$ )

Sample	Added value (CFU mL <sup>-1</sup> )	Detected (CFU mL <sup>-1</sup> )	Recovery (%)	RSD (%)
1	10 <sup>2</sup>	9.93 × 10 <sup>1</sup> (± 0.04)	99.3	4.5
2	10 <sup>4</sup>	1.007 × 10 <sup>4</sup> (± 0.13)	100.7	4.8
3	10 <sup>6</sup>	1.068 × 10 <sup>6</sup> (± 0.05)	106.8	5.7

### *A. baumannii* measurement in real samples

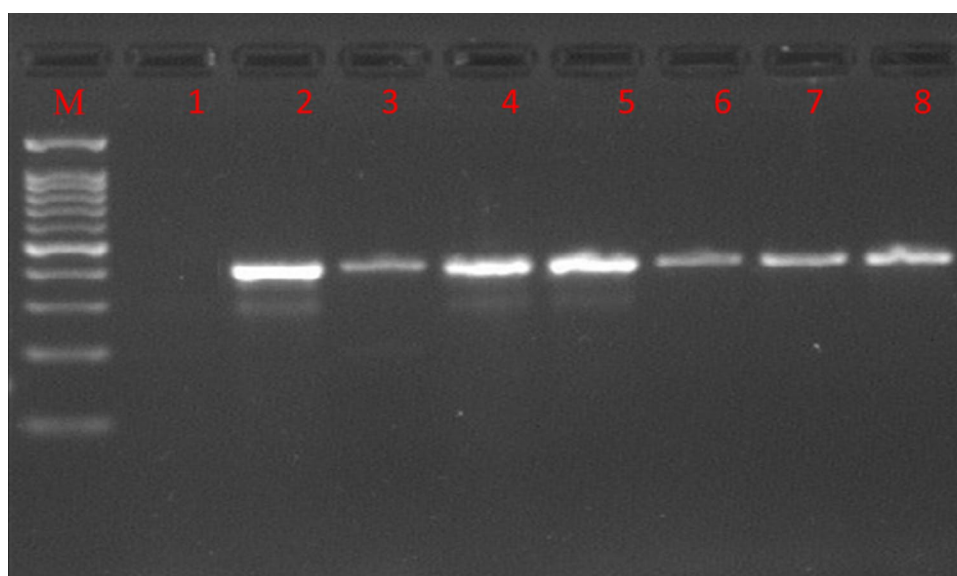
Measuring the real sample is an important factor in the electrochemical sensor. Human blood serum samples

were prepared from a local clinical laboratory to evaluate the application of the proposed measurement system for real sample analysis. EIS technique and the standard addition method were used for *A. baumannii* detection. During the first step, the concentration of *A. baumannii* was adjusted to 0.5 McFarland turbidity. The blood serum sample was then diluted 5 times with PB solutions (0.1 M, pH 7.4). Afterward, we spiked the diluted serum samples with different concentrations of *A. baumannii* 10<sup>2</sup>, 10<sup>4</sup> and 10<sup>6</sup> CFU mL<sup>-1</sup>. The obtained recoveries for the spiked antigen concentrations were in the range of 99.3 to 106.8%. The results in Table 2 show that, in this study, a sensor can be used to identify *A. baumannii* in real samples. In addition, PCR was performed for sensor validation as well as its sensitivity, Fig. 7.

### Conclusion

In this study, the modified electrochemical sensor with PDA imprinted film for simple, rapid and direct detection of *A. baumannii* has been developed for the first time. The PDA copolymer which modified the electrochemical sensor gave powerful polymer capacity and performance. The cavities made in the imprinted films represent a favorable selection of *A. baumannii*. In addition, this method is very easy to be prepared and can be used as a simple diagnostic method for other bacteria.

**Fig. 7** PCR detection of the O-antigen acetylase gene in *A. baumannii*. The presence of the 400 bp amplicon indicates positive result for *A. baumannii* at different concentrations: lane M, 100 bp DNA size marker; lane 1, negative control; lane 2, positive control; lane 3, 10<sup>2</sup> CFU mL<sup>-1</sup>; lane 4, 10<sup>3</sup> CFU mL<sup>-1</sup>; lane 5, 10<sup>4</sup> CFU mL<sup>-1</sup>; lane 6, 10<sup>5</sup> CFU mL<sup>-1</sup>; lane 7, 10<sup>6</sup> CFU mL<sup>-1</sup>; and lane 8, 10<sup>7</sup> CFU mL<sup>-1</sup>



**Acknowledgement** This study has been supported by the Ilam University.

## References

1. L. Dijkshoorn, A. Nemeč, H. Seifert, *Nat. Rev. Microbiol.* **5**, 939 (2007)
2. P.E. Fournier, H. Richet, R.A. Weinstein, *Clin. Infect. Dis.* **42**, 692–699 (2006)
3. E. Pérez-Trallero, J.E. Martín-Herrero, A. Mazón, C. García-Delafuente, P. Robles, V. Iriarte, R. Dal-Ré, J. García-de-Lomas, *Antimicrob. Agents Chemother.* **54**, 2953–2959 (2010)
4. A. Potron, L. Poiriel, P. Nordmann, *Int. J. Antimicrob. Agents* **45**, 568–585 (2015)
5. L. Antunes, P. Visca, K.J. Towner, *Pathog. Dis.* **71**, 292–301 (2014)
6. S. Göttig, T.M. Gruber, P.G. Higgins, M. Wachsmuth, H. Seifert, V.A.J. Kempf, *J. Antimicrob. Chemother.* **69**, 2578–2579 (2014)
7. J.F. Turton, N. Woodford, J. Glover, S. Yarde, M.E. Kaufmann, T.L. Pitt, *J. Clin. Microbiol.* **44**, 2974–2976 (2006)
8. M. Kempf, S. Bakour, C. Flaudrops, M. Berrazeg, J.-M. Brunel, M. Drissi, E. Mesli, A. Touati, J.-M. Rolain, *PLoS ONE* **7**, e31676 (2012)
9. Y. Zheng, X. Wang, H. Jiang, *Sensors Actuators B Chem.* **277**, 388–393 (2018)
10. Y. Liu, Y. Liang, R. Yang, J. Li, L. Qu, *Talanta* **195**, 691–698 (2019)
11. M.A. Hammam, H.A. Wagdy, R.M. El Nashar, *Sensors Actuators B Chem.* **275**, 127–136 (2018)
12. X. Zhang, S. Yang, L. Sun, A. Luo, *J. Mater. Sci.* **51**, 6075–6085 (2016)
13. Z.-Z. Yin, S.-W. Cheng, L.-B. Xu, H.-Y. Liu, K. Huang, L. Li, Y.-Y. Zhai, Y.-B. Zeng, H.-Q. Liu, Y. Shao, *Biosens. Bioelectron.* **100**, 565–570 (2018)
14. P. Wang, X.F. Fu, J. Li, J. Luo, X.Y. Zhao, M.J. Sun, Y.Z. Shang, C. Ye, *Chin. Chem. Lett.* **22**, 611–614 (2011)
15. S. Ansari, *TrAC Trends Anal. Chem.* **93**, 134–151 (2017)
16. A.G. Mayes, K. Mosbach, *TrAC Trends Anal. Chem.* **16**, 321–332 (1997)
17. H. Peng, C. Liang, A. Zhou, Y. Zhang, Q. Xie, S. Yao, *Anal. Chim. Acta* **423**, 221–228 (2000)
18. P. Liu, X. Zhang, W. Xu, C. Guo, S. Wang, *Sensors Actuators B Chem.* **163**, 84–89 (2012)
19. X. Zhang, X. Du, X. Huang, Z. Lv, *J. Am. Chem. Soc.* **135**, 9248–9251 (2013)
20. Y. Yu, Q. Zhang, J. Buscaglia, C.-C. Chang, Y. Liu, Z. Yang, Y. Guo, Y. Wang, K. Levon, M. Rafailovich, *Analyst* **141**, 4424–4431 (2016)
21. Y. Yu, Q. Zhang, C.-C. Chang, Y. Liu, Z. Yang, Y. Guo, Y. Wang, D.K. Galanakis, K. Levon, M. Rafailovich, *Analyst* **141**, 5607–5617 (2016)
22. K. Liu, W.-Z. Wei, J.-X. Zeng, X.-Y. Liu, Y.-P. Gao, *Anal. Bioanal. Chem.* **385**, 724–729 (2006)
23. C.-H. Su, M.-H. Tsai, C.-Y. Lin, Y.-D. Ma, C.-H. Wang, Y.-D. Chung, G.-B. Lee, *Biosens. Bioelectron.* **159**, 112148 (2020)
24. Y.-L. Bai, M. Shahed-Al-Mahmud, K. Selvaprakash, N.-T. Lin, Y.-C. Chen, *Anal. Chem.* **91**, 10335–10342 (2019)